Mathematical Model of the Biosensors Acting in a Trigger Mode

Romas Baronas [1,*], Juozas Kulys [2] and Feliksas Ivanauskas [1,3]

[1] Faculty of Mathematics and Informatics, Vilnius University, Naugarduko 24, 2006 Vilnius, Lithuania

[2] Vilnius Gediminas Technical University, Sauletekio Avenue 11, 2040 Vilnius, Lithuania

[3] Institute of Mathematics and Informatics, Akademijos 4, 2600 Vilnius, Lithuania

* Author to whom correspondence should be addressed. E-mail: romas.baronas@maf.vu.lt

Abstract: A mathematical model of biosensors acting in a trigger mode has been developed. One type of the biosensors utilized a trigger enzymatic reaction followed by the cyclic enzymatic and electrochemical conversion of the product (CCE scheme). Other biosensors used the enzymatic trigger reaction followed by the electrochemical and enzymatic product cyclic conversion (CEC scheme). The models were based on diffusion equations containing a non-linear term related to Michaelis-Menten kinetics of the enzymatic reactions. The digital simulation was carried out using the finite difference technique. The influence of the substrate concentration, the maximal enzymatic rate as well as the membrane thickness on the biosensor response was investigated. The numerical experiments demonstrated a significant gain (up to dozens of times) in biosensor sensitivity when the biosensor response was under diffusion control. In the case of significant signal amplification, the response time with triggering was up to several times longer than that of the biosensor without triggering.

Introduction

The chemical amplification in analysis was reviewed almost 25 years ago [1]. The sensitivity of biosensors can be increased by chemical amplification, too. The amplification in the biosensors response was achieved by the cyclic conversion of substrates [2-8]. The cyclic conversion of the substrate and the regeneration of the analyte are usually performed by using a membrane containing two enzymes. The calculations of the steady-state response of the enzyme electrodes with cyclic substrate conversion were performed under the first-order reaction conditions [2]. Dynamic response of these electrodes was analysed by solving diffusion equations and using Green's function [9]. Further analysis of the dual enzyme biosensors response was performed by Schulmeister and others [4,10-12].

The substrate cyclic conversion by conjugating the enzymatic reaction with chemical or electrochemical process was utilized in a single enzyme membrane [3,13-15]. Digital modelling of this type of biosensors was performed only recently [16].

If a biosensor contains an enzyme that starts analyte conversion followed by cyclic product conversion, the scheme of the biosensor action can be called a "triggering". An example of this type of conversion is the amperometric detection of alkaline phosphatase based on hydroquinone recycling [17]. The substrate of the alkaline phosphatase, i.e. p-hydroxyphenyl phosphate, is hydrolysed by alkaline phosphatase to hydroquinone. The hydroquinone, instead of being detected directly, enters an amplification cycle where it is oxidized to quinone at the electrode surface and then reduced back to hydroquinone by glucose oxidase in the presence of glucose. The consumption-regeneration cycle of hydroquinone results in an amplification factor of about 8. Another example utilizing trigger scheme is the highly sensitive determination of β-galactosidase used as a label in a heterogeneous immunoassay [18]. As a substrate, *p*-aminophenyl- β-galactopyranoside was used. The produced *p*-aminophenol, which is an electrochemically active compound, can be detected directly [19]. To increase the sensitivity of the determination, *p*-aminophenol is entered into a bioelectrocatalytic amplification cycle by using glucose dehydrogenase (GDH). Both schemes presented include enzymatic trigger reactions together with electrochemical and enzymatic amplification steps. Therefore, by analogy with an electrochemical nomenclature, they may be abbreviated as acting by the CEC mechanism.

The triggering of the consecutive substrate conversion can also be realized by enzymatic conversion of the substrate (trigger reaction) followed by the second enzymatic reaction and electrochemical conversion. This scheme can be abbreviated as CCE. The scheme may be realized, for example, by using peroxidase and glucose dehydrogenase. The peroxidase produces an oxidized product that is reduced by GDH, thus realizing the cyclic conversion of the product. The goal of this investigation is to propose a model allowing computer simulation of the biosensor response utilising both schemes. The model developed is based on non-stationary diffusion equations [20], containing a non-linear term related to the enzymatic reaction. The digital simulation of the biosensor response was carried out by using the implicit finite difference scheme [21-23]. The program developed was employed to investigate the influence of the substrate concentration, the maximal enzymatic rate as well as the membrane thickness on the biosensor response.

Mathematical Models

A biosensor is considered as an enzyme electrode, containing a membrane with immobilised enzymes applied onto the surface of the electrochemical transducer. We assume the symmetrical geometry of the electrode and homogeneous distribution of immobilised enzymes in the enzyme membrane.

Model of biosensors in CEC mode

In the CEC scheme, the substrate (S) is enzymatically (E$_1$) converted to the product (P$_1$) followed by the electrochemical conversion of the product (P$_1$) to another product (P$_2$) that, in turn, is enzymatically (E$_2$) converted back to P$_1$:

$$S \xrightarrow{\text{E}_1} P_1 \tag{1}$$

$$P_1 \longrightarrow P_2 \tag{2}$$

$$P_2 \xrightarrow{\text{E}_2} P_1 \tag{3}$$

Coupling the enzyme-catalysed reactions (1), (3) and electrochemical reaction (2) with the one-dimensional-in-space diffusion, described by Fick's law, leads to the following equations ($t > 0$, $0 < x < d$):

$$\frac{\partial S}{\partial t} = D_\text{S} \frac{\partial^2 S}{\partial x^2} - \frac{V_1 S}{K_1 + S} \tag{4}$$

$$\frac{\partial P_1}{\partial t} = D_{\text{P}_1} \frac{\partial^2 P_1}{\partial x^2} + \frac{V_1 S}{K_1 + S} + \frac{V_2 P_2}{K_2 + P_2} \tag{5}$$

$$\frac{\partial P_2}{\partial t} = D_{\text{P}_2} \frac{\partial^2 P_2}{\partial x^2} - \frac{V_2 P_2}{K_2 + P_2} \tag{6}$$

where x and t stand for space and time, respectively, $S(x,t)$ and $P_i(x,t)$ denote the concentration functions of the substrate S and product P$_i$, respectively, V_i is the maximal enzymatic rate, K_i is the Michaelis constant, d is the thickness of the enzyme membrane, D_S and D_{P_i} are the diffusion coefficients, $i = 1, 2$.

Let $x = 0$ represent the electrode surface and $x = d$ the bulk solution/membrane interface. The operation of the biosensor starts when some substrate appears over the surface of the enzyme membrane. This is used with the initial conditions ($t = 0$):

$$S(x,0) = 0, \quad 0 \le x < d, \qquad S(d,0) = S_0 \tag{7}$$

$$P_i(x,0) = 0, \quad 0 \le x \le d, \quad i = 1, 2 \tag{8}$$

where S_0 is the concentration of substrate in the bulk solution.

The electrode potential is chosen to keep the zero concentration of the product P$_1$ at the electrode surface. The rate of the product P$_2$ generation at the electrode is proportional to the rate of conversion of the product P$_1$. When the substrate is well-stirred outside the membrane, the diffusion layer remains at a constant thickness ($0 < x < d$). Consequently, the concentration of the substrate as well as both

products over the enzyme surface (bulk solution/membrane interface) remains constant while the biosensor contacts the solution of substrate. This is used in the boundary conditions ($t > 0$) given by

$$\left.\frac{\partial S}{\partial x}\right|_{x=0} = 0 \tag{9}$$

$$S(d,t) = S_0 \tag{10}$$

$$D_{P_2}\left.\frac{\partial P_2}{\partial x}\right|_{x=0} = -D_{P_1}\left.\frac{\partial P_1}{\partial x}\right|_{x=0} \tag{11}$$

$$P_i(d,t) = 0, \quad i = 1, 2 \tag{12}$$

$$P_1(0,t) = 0 \tag{13}$$

The biosensor current depends upon the flux of the product P_1 at the electrode surface, i.e. at the border $x = 0$. Consequently, the density $i_{CEC}(t)$ of the current at time t can be obtained explicitly from Faraday's and Fick's laws using the flux of the concentration P_1 of the product P_1 at the surface of the electrode

$$i_{CEC}(t) = n_e F D_{P_1}\left.\frac{\partial P_1}{\partial x}\right|_{x=0} = -n_e F D_{P_2}\left.\frac{\partial P_2}{\partial x}\right|_{x=0} \tag{14}$$

where n_e is the number of electrons involved in a charge transfer at the electrode surface, and F is the Faraday constant, $F = 96485$ C/mol.

We assume, that system (4)-(14) approaches a steady-state as $t \to \infty$:

$$I_{CEC} = \lim_{t \to \infty} i_{CEC}(t) \tag{15}$$

where I_{CEC} is the steady-state biosensor current.

Model of biosensors in CCE mode

In the CCE scheme, the substrate (S) is enzymatically (E_1) transformed to the product (P_1) followed by the enzymatic (E_2) conversion of the product P_1 to another product P_2 that, in turns, is electrochemically converted back to P_1:

$$S \xrightarrow{\ E_1\ } P_1 \tag{16}$$

$$P_1 \xrightarrow{\ E_2\ } P_2 \tag{17}$$

$$P_2 \longrightarrow P_1 \tag{18}$$

If the thickness of enzyme membrane is d, coupling of reactions (16)-(18) with the diffusion leads to the following equations ($t > 0$, $0 < x < d$):

$$\frac{\partial S}{\partial t} = D_S \frac{\partial^2 S}{\partial x^2} - \frac{V_1 S}{K_1 + S} \tag{19}$$

$$\frac{\partial P_1}{\partial t} = D_{P_1} \frac{\partial^2 P_1}{\partial x^2} + \frac{V_1 S}{K_2 + S} - \frac{V_2 P_1}{K_2 + P_1} \tag{20}$$

$$\frac{\partial P_2}{\partial t} = D_{P_2} \frac{\partial^2 P_2}{\partial x^2} + \frac{V_2 P_1}{K_2 + P_1} \qquad (21)$$

Here and below, all the symbols have the same meaning as in the model above. The initial conditions are described by (7), (8) exactly as in the case of CEC scheme.

When the biosensor acts in the CCE mode, the electrode potential is chosen to keep zero concentration of the product P_2 at the electrode surface. The rate of the product P_1 generation at the electrode is proportional to the rate of conversion of the product P_2. Consequently, the boundary conditions (9)-(12) are also applicable to the system (16)-(18). Only one of the boundary conditions (13) of the system acting in the CEC mode has to be replaced by the following condition:

$$P_2(0,t) = 0 \qquad (22)$$

The density $i_{CCE}(t)$ of the biosensor current is proportional to the concentration gradient of the product P_2 at the surface of the electrode:

$$i_{CCE}(t) = n_e F D_{P_2} \frac{\partial P_2}{\partial x}\bigg|_{x=0} = -n_e F D_{P_1} \frac{\partial P_1}{\partial x}\bigg|_{x=0}. \qquad (23)$$

When the system (19)-(21), (7)-(12), (22) approaches a steady-state, we obtain the steady-state current I_{CCE} of the biosensor acting in CCE mode

$$I_{CCE} = \lim_{t \to \infty} i_{CCE}(t) \qquad (24)$$

Model of biosensors in CE mode

To compare the responses of trigger and normal biosensors, the action of the CE biosensor was analysed. In accordance to the CE scheme, the substrate (S) is enzymatically (E_1) converted to the product (P_1) followed by the electrochemical product (P_1) conversion to another product (P_2):

$$S \xrightarrow{\ E_1\ } P_1 \qquad (25)$$

$$P_1 \longrightarrow P_2 \qquad (26)$$

The mathematical model of a biosensor acting in CE mode can be derived from the model (4)-(13) of a biosensor acting in CEC mode by accepting an inactive enzyme E_2, i.e. $V_2 = 0$. If $i_{CE}(t)$ is assumed to be the current of a biosensor acting in CE mode, it can be calculated by (14), while the steady-state current I_{CE} by (15). This type of biosensors is widespread [24].

The enzymatic amplification in a trigger mode

To compare the amplified biosensor response with the response without amplification, we define the gain of the sensitivity as the ratio of the steady-state current of the trigger biosensor to the steady-state current of a corresponding CE biosensor

$$G_{CEC}(V_1, V_2) = \frac{I_{CEC}(V_1, V_2)}{I_{CE}(V_1)} = \frac{I_{CEC}(V_1, V_2)}{I_{CEC}(V_1, 0)}, \qquad (27)$$

$$G_{\text{CCE}}(V_1, V_2) = \frac{I_{\text{CCE}}(V_1, V_2)}{I_{\text{CE}}(V_1)} = \frac{I_{\text{CCE}}(V_1, V_2)}{I_{\text{CEC}}(V_1, 0)} \tag{28}$$

where $I_{\text{CEC}}(V_1, V_2)$ and $I_{\text{CCE}}(V_1, V_2)$ are the steady-state currents of the trigger biosensors acting in CEC and CCE mode, respectively, at the maximal activity V_i of an enzyme E_i, $i = 1, 2$, $I_{\text{CE}}(V_1)$ is the steady-state current of the corresponding CE biosensor measured at the maximal enzymatic rate V_1 of an enzyme E_1, and $I_{\text{CE}}(V_1) = I_{\text{CEC}}(V_1, 0)$.

Digital Simulation

Definite problems arise when solving analytically the non-linear partial differential equations with complex boundary conditions [20,21]. To obtain an approximate analytical solution, approximation and classification of each condition is needed. On the other hand, digital simulation can be applied almost in any case and usually neither simplification nor classification is necessary. Consequently, the mathematical models were solved numerically for both CEC and CCE systems. The system acting in CE model was treated as a particular case of the CEC system with $V_2 = 0$.

The finite difference technique [25] was applied to discretize the mathematical models. We introduced a uniform discrete grid in both x and t directions. Implicit linear finite difference schemes have been built as a result of the difference approximation of the models. The resulting systems of linear algebraic equations were solved efficiently because of the tridiagonality of the matrices of the systems [16,24].

An explicit scheme is easier to program, however, the implicit one is more efficient [21-23]. Although the processing speed of modern computers is high enough to ensure the practical use of explicit schemes, the use of the faster implicit scheme is well justified because of a large number of simulations which were carried out in the investigation discussed below.

Due to the boundary conditions (9)-(13) and (22), a small step of the grid was required in x direction in order to have an accurate and stable result of computations [20,25]. Usually, an implicit computational scheme does not restrict time increment. However, the step size of the grid in time direction was restricted due to the non-linear reaction term in (4)-(6), (19)-(21), and boundary conditions. In order to be accurate, we employed a space step size of $10^{-3}d$. The steady-state time of membrane biosensors significantly depends on the thickness of the enzyme layer [24]. The steady-state time varies even in orders of magnitude. Because of this, we assume that the time step size τ is directly proportional to the membrane thickness d, $\tau = kd$. To obtain an accurate biosensor current in the entire domain of simulation time $t > 0$, we employed $k = 0.1$ s/cm. However, for an accurate simulation of the steady-state current, only $k = 10$ s/cm was enough. The program was written in C language [26].

In digital simulation, the biosensor steady-state time was defined as the time when the absolute current slope value falls below a given small value normalised with the current value. In other words, the time needed to achieve a given dimensionless decay rate ε is used:

$$T_m = \min_{i_m(t) > 0} \left\{ t : \frac{1}{i_m(t)} \left| \frac{\partial i_m(t)}{\partial t} \right| < \varepsilon \right\}, \quad m = \text{CEC, CCE} \tag{29}$$

Consequently, the steady-state biosensor currents I_{CEC} and I_{CCE} were taken as the current at the biosensor response time T_{CCE} and T_{CCE}, respectively, $I_{CEC} \approx i_{CEC}(T_{CEC})$, $I_{CCE} \approx i_{CCE}(T_{CCE})$. In calculations, we used $\varepsilon = 10^{-5}$.

The mathematical models as well as the numerical solutions of the models were evaluated for different values of the maximal enzymatic rates V_1 and V_2, substrate concentration S_0, and thickness d of the enzyme layer. The following values of the parameters were constant in the numerical simulation of all the experiments [15]:

$$D_S = D_{P_1} = D_{P_2} = 3.0 \times 10^{-6} \, \text{cm}^2 / \text{s}$$
$$K_1 = K_2 = 10^{-7} \, \text{mol/cm}^3, \quad n_e = 2 \tag{30}$$

Results and Discussion

The compounds concentration in the enzyme membrane

In Figs. 1 and 2, the profiles of substrate as well as product concentration in the enzyme layer are presented for biosensors acting in CEC and CCE modes. For calculations, the maximal enzymatic rate $V_1 = V_2 = 100 \, \text{nmol/(cm}^3\text{s)}$, substrate concentration $S_0 = 20 \, \text{nmol/cm}^3$ and membrane thickness $d = 0.01$ cm were used. The profiles show the concentrations normalized to the Michaelis constant K_M, assuming $K_M = K_1 = K_2 = 5S_0$, $S_{0N} = 0.2$:

$$S_{0N} = S_0/K_M, \quad S_N = S/K_M, \quad P_{1N} = P_1/K_M, \quad P_{2N} = P_2/K_M \tag{31}$$
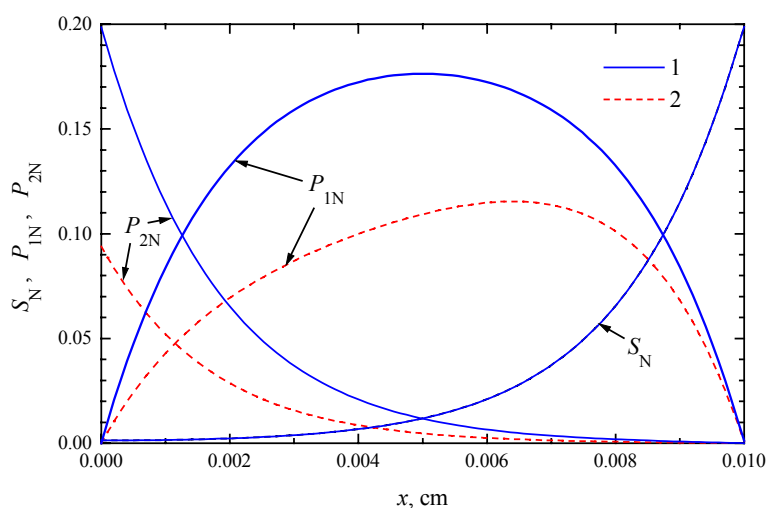
Figure 1. The profiles of the normalized concentrations of substrate (S_N) and products (P_{1N}, P_{2N}) in the enzyme membrane of a CEC biosensor at the maximal enzymatic rate $V_1 = V_2 = 100$ nmol/(cm^{3}s), $S_{0N} = 0.2$, $d = 0.01$ cm. The profiles show the concentrations at the steady-state time $t = 123$ s (1) and half time $t = 12$ s (2).

The concentration profiles in Figs. 1, 2 are shown at the time when the steady-state as well as 50% of the steady-state response has been reached. Note that for both biosensors the concentration of the substrate at steady-state conditions is approximately the same. At the time when the half of the steady-

state response is reached, no significant difference has been observed, too. This is true in the entire enzyme layer, $x \in [0, d]$. The substrate concentration is described by equations (4), (7), (9) and (10), which are valid in both modes of biosensor action. This explains the similarity of substrate concentration in both modes.
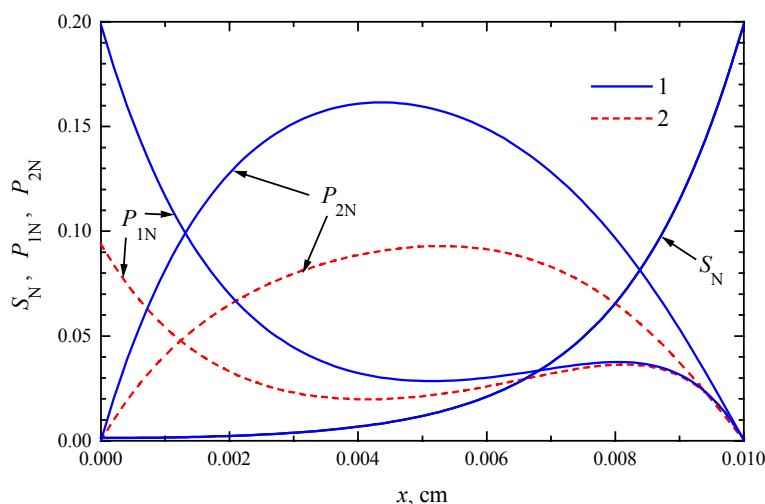
Figure 2. The profiles of the normalized concentrations in the enzyme membrane of a CCE biosensor at time $t = 124$ s (1) when the steady-state is reached and $t = 12$ s (2) at the half of it. Other parameters and notation are the same as in Fig. 1.

The steady-state current is similar for both types of biosensors, $I_{CEC} \approx i_{CEC}(123) \approx 6.23$ µA/cm^2, $I_{CCE} \approx i_{CCE}(124) \approx 6.09$ µA/cm^2. The time of steady-state is also approximately the same in both these cases. At the steady-state conditions, i.e. $\partial S / \partial t = \partial P_1 / \partial t = \partial P_2 / \partial t = 0$, because of the boundary conditions (9)-(12), the equality $S(x, t) + P_1(x, t) + P_2(x, t) = S_0$ holds for all $x \in [0, d]$ when $t \to \infty$. This can be observed in both Figs. 1 and 2.

The dependence of the steady-state current on the reactions rates

The dependence of the steady-state current on the activity of both enzymes is shown in Figs. 3, 4 for CEC and CCE modes. In calculations, V_1 and V_2 varied from 10^{-10} to 10^{-6} mol/(cm^{3}s), the substrate concentration S_0 was 20 nmol/cm^3, S_{0N} was 0.2 and membrane thickness d was 0.01 cm. One can see in Figs. 3 and 4 that $I_{CEC}(V_1, V_2)$ as well as $I_{CCE}(V_1, V_2)$ are monotonously increasing functions of both arguments: V_1 and V_2.

In the case of CEC mode, an application of an active enzyme E$_2$ ($V_2 > 0$) stimulates an increase of the biosensor current. In the case of $V_2 = 0$, the biosensor acting in CEC mode generates the current if only $V_1 > 0$. However, in the case of CCE mode, the appearance of an active enzyme E$_2$ ($V_2 > 0$) is a critical factor for the biosensor current. $I_{CCE} = 0$ if $V_2 = 0$ even if the activity of an enzyme E$_1$ is very high ($V_1 \gg 0$). Because of this, at low values of V_2, the steady-state current I_{CCE} increases very quickly with increase of V_2. That effect is noted in Figs. 3 and 4 as the surface salience. The salience of the surface $I_{CCE}(V_1, V_2)$ (Fig. 4) is more noticeable than the salience of the surface $I_{CEC}(V_1, V_2)$ (Fig. 3).
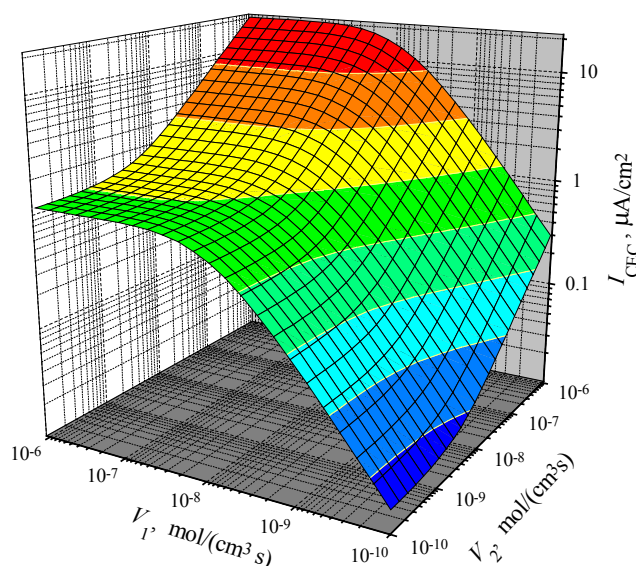
Figure 3. The steady-state current versus the maximal enzymatic rates V_1 and V_2 of the biosensor acting in CEC mode, $S_{0N} = 0.2$, $d = 0.01$ cm.

Consequently, when $V_2 \to 0$ at any $V_1 > 0$, in the CEC mode: $I_{CCE}(V_1, V_2) \to 0$, while in another mode (CEC) of triggering: $I_{CEC}(V_1, V_2) \to I_{CEC}(V_1, 0) = I_{CE}(V_1)$. On the other hand, Figs. 3 and 4 show, that $I_{CEC}(V_1, V_2) \approx I_{CCE}(V_1, V_2)$ at a high maximal enzymatic rate V_2.
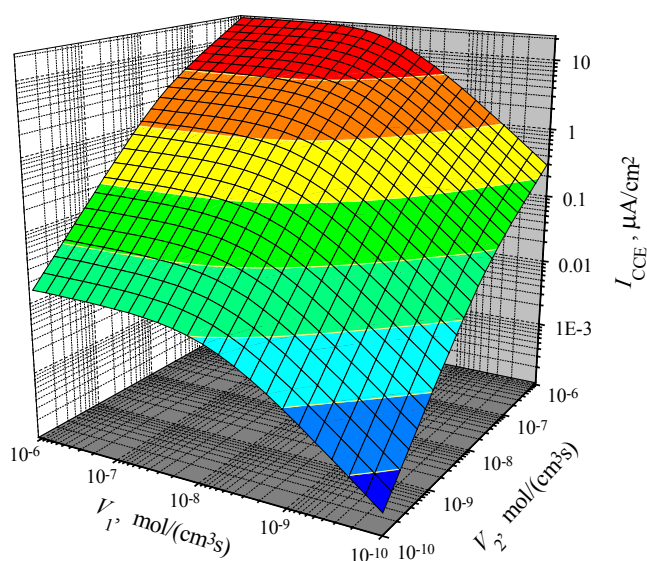

Figure 4. The steady-state current versus V_1 and V_2 of the biosensor acting in CCE mode at the same conditions as in Fig. 3.

*The dependence of the amplification on the reactions rates*

To investigate the effect of the amplification, $I_{CE}(V_1)$ has been calculated at the same conditions as above. Having $I_{CEC}(V_1, V_2)$, $I_{CCE}(V_1, V_2)$ and $I_{CE}(V_1)$, we calculated the gains $G_{CEC}(V_1, V_2)$ and $G_{CCE}(V_1, V_2)$. Results of calculations are depicted in Figs. 5 and 6. One can see in both figures that the gain increases with increase of V_2. The increase is especially notable at high values of V_2. The variation of

V_1 on the response gain is slight by only. The gain varies from 18.0 to 19.1 at $V_2 = 1$ μmol/(cm³s) in both action modes: CEC and CCE.

Comparing the gain in the CEC mode (Fig. 5) with the gain in the CCE mode (Fig. 6), one can notice a significant difference at low values of V_2. The gain G_{CEC} starts to increase from about unity, while G_{CCE} at low values of V_2 ($V_2 < \approx 1$ nmol/(cm³s)) is even less than unity. It means that in the case of low activity of enzyme E_2, the steady-state current of a biosensor is acting in the CCE mode even less than the steady-state current of a biosensor acting in the CE mode at the same conditions.
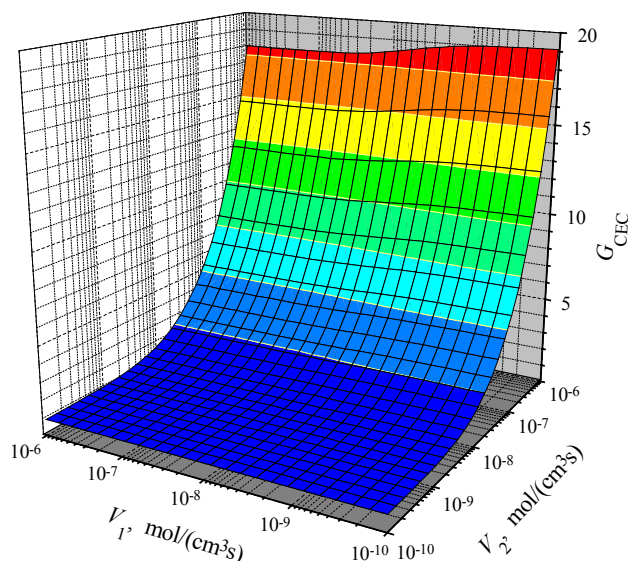
Figure 5. The signal gain G_{CEC} versus the maximal enzymatic rates V_1 and V_2 of the biosensor acting in the CEC mode at the conditions defined in Fig. 3.
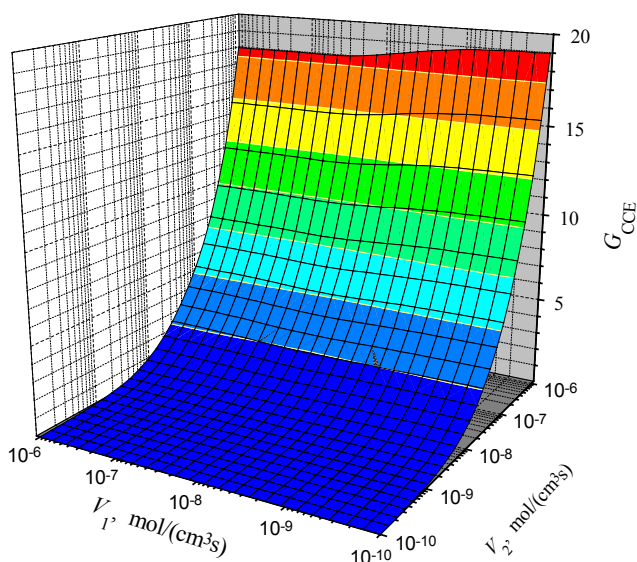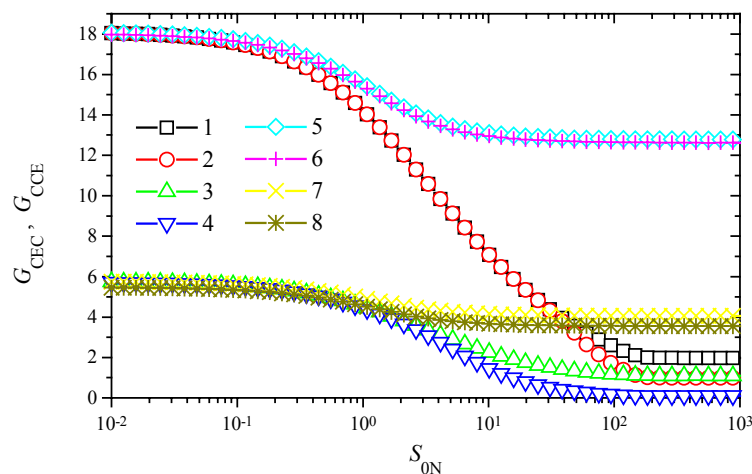

Figure 6. The signal gain G_{CCE} versus the maximal enzymatic rates V_1 and V_2 of the biosensor acting in the CCE mode at the conditions defined in Fig. 3.

From the model of the CCE biosensor follows that $P_2(x, t) \approx 0$ when $V_2 \rightarrow 0$. Consequently, $G_{CCE}(V_1, V_2) \rightarrow 0$ when $V_2 \rightarrow 0$ at any $V_1 > 0$, while in the CEC mode: $G_{CEC}(V_1, V_2) \rightarrow 1$ when $V_2 \rightarrow 0$.

On the other hand, Figs. 5 and 6 show, that $G_{CEC}(V_1, V_2) \approx G_{CCE}(V_1, V_2)$ at a high maximal enzymatic rate V_2, e.g. at $V_2 = 1$ µmol/(cm^{3}s).

The dependence of the amplification on the substrate concentration

To investigate the dependence of the signal gain on the substrate concentration S_0, the response of biosensors varying S_0 from 10^{-10} to 10^{-4} mol/cm^3 was simulated. Since the gain of trigger biosensors is significant only at a relatively high maximal enzymatic rate V_2 of enzyme E_2 (Figs. 5 and 6), we employed the following two values of V_2: 10^{-6} and 10^{-7} mol/(cm^{3}s). We chose also two different values of the maximal enzymatic rate V_1 of enzyme E_1: 10^{-6} and 10^{-8} mol/(cm^{3}s). Since the influence of V_1 on the signal gain is not so significant as that of V_2, the chosen two values of V_1 differ in two orders of magnitude while values of V_2 differ only in one. The results of calculations at the enzyme membrane thickness $d = 0.01$ cm are depicted in Fig. 7.

Figure 7. The signal gains G_{CEC} (1, 3, 5, 7) and G_{CCE} (2, 4, 6, 8) vs. the substrate concentration S_{0N} at the maximal enzymatic rates V_1: 100 (1-4), 1 (5-8) and V_2: 100 (1, 2, 5, 6), 10 (3, 4, 7, 8) nmol/(cm^{3}s), $d = 0.01$ cm.

As one can see in Fig. 7, the behaviour of the signal gain versus the substrate concentration is very similar for both modes of the biosensor action: CEC and CCE. Some noticeable difference between values of G_{CEC} and G_{CCE} is observed at high substrate concentrations only, $S_{0N} > 1$. However, in a case of a higher value of V_2, $V_2 = 10^{-6}$ mol/(cm^{3}s), and a lower V_1, $V_1 = 10^{-8}$ mol/(cm^{3}s), no noticeable difference is observed between values of G_{CEC} (curve 5 in Fig. 7) and G_{CCE} (curve 6 in Fig. 7) in the entire domain of substrate concentration. A very similar effect can be noticed at the same value of V_1, $V_1 = 10^{-6}$ mol/(cm^{3}s), and a ten times higher value of V_2, $V_2 = 10^{-7}$ mol/(cm^{3}s), curves 7 and 8.

Fig. 7 shows the significant importance of the maximal enzymatic rate V_2 to both signal gains: G_{CEC} and G_{CCE}. Such an importance is especially perceptible at low and moderate concentrations of substrate, $S_{0N} < 1$. At $S_{0N} < 0.1$ and $V_2 = 1$ µmol/(cm^{3}s) due to the amplification, the steady-state current increases up to about 18 times ($G_{CEC} \approx G_{CCE} \approx 18$). However, at the same S_{0N} and ten times lower value of V_2, the gain is about three times less, $G_{CEC} \approx G_{CCE} \approx 5.7$. Consequently, at low substrate

concentrations, $S_{0N} < 0.1$, and wide range of the maximal enzymatic rate V_1, the tenfold reduce of V_2 reduces the signal gain about three times. This property is valid for both modes of triggering: CEC and CCE.

When increasing the substrate concentration, the signal gain starts to decrease when S_{0N} becomes greater than unity (Fig. 7), i.e. when $S_0 > K_1 = K_2$. However, the decrease is perceptible in cases of a high enzymatic rate V_1 only. At low activity of enzyme E_1 when $V_1 = 1$ nmol/(cm^{3}s), the gain varies less than 30% for both values of V_2: 10 and 100 nmol/(cm^{3}s). Additional calculations showed, that at a less activity of enzyme E_1 when $V_1 = 10^{-10}$ mol/(cm^{3}s), the gain practically does not vary changing the substrate concentration in the domain. Because of a very stable amplification at a wide range of substrate concentration, the usage of biosensors acting in a trigger mode is especially reasonable at a relatively low maximal enzymatic activity (rate V_1) of enzyme E_1 and a high activity (rate V_2) of enzyme E_2. In the cases of relatively high maximal enzymatic activity V_1 the signal amplification is stable only for low concentrations of the substrate.

Additional calculations showed that the signal gain vanishes fast with the decrease of the enzymatic activity V_2 of enzyme E_2. For example, in the case of $V_2 = 1$ nmol/(cm^{3}s) the gain becomes less than 2 even at a low substrate concentration, $G_{CEC} \approx 1.91$, $G_{CCE} \approx 1.3$ at $S_{0N} = 0.01$. This effect is also observed in Figs. 5 and 6. Calculations approved the property that the tenfold reduce of V_2 reduces the signal gain about three times is valid at a wide range, also of V_2.

A similar dependence of the signal gain on the substrate concentration was observed in the case of an amperometric enzyme electrode with immobilized laccase, in which a chemical amplification by cyclic substrate conversion takes place in a single enzyme membrane [15]. In the case of the biosensor with substrate cyclic conversion, the signal gain of 36 times was observed at the maximal enzymatic rate of 1 µmol/(cm^{3}s) and the membrane thickness of 0.02 cm. For comparison of that gain with the gain achieved in the trigger mode, we calculate G_{CEC} and G_{CCE} for the enzyme membrane of thickness $d = 0.02$ cm. The result of the calculation showed the amplification, $G_{CEC} \approx G_{CCE} \approx 34$ at $V_1 = V_2 = 1$ µmol/cm^{3}s, $d = 0.02$ cm, very similar to the amplification noticed in [15,16].

The effect of the enzyme membrane thickness on the amplification

The steady-state current of membrane biosensors significantly depends on the thickness of the enzyme layer [6,16,24,27]. The steady-state time varies even in orders of magnitude. To investigate the dependence of the signal gain on the membrane thickness d, the response of biosensors varying d from 0.0001 to 0.05 cm at different maximal enzymatic rate V_1 of enzyme E_1 and rate V_2 of enzyme E_2 was simulated.
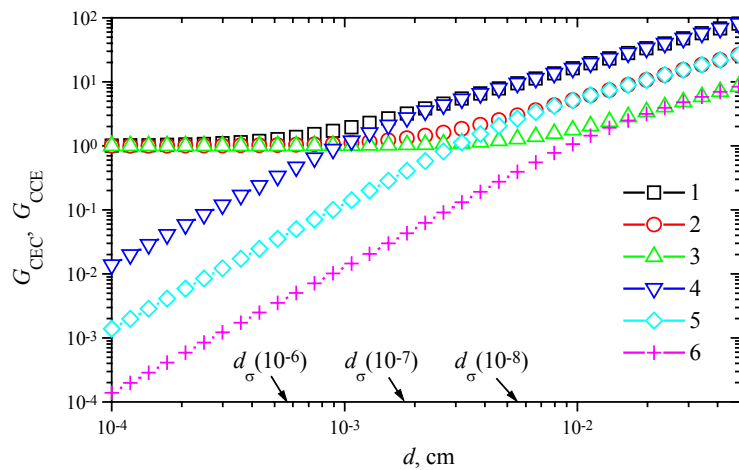
Fig. 8 shows the signal gains G_{CEC} and G_{CCE} versus the membrane thickness d at the maximal enzymatic rate $V_1 = 1$ µmol/(cm^{3}s) and three values of the rate V_2: 1, 10 and 100 nmol/(cm^{3}s). Comparing the gain G_{CEC} with G_{CCE}, one can notice valuable differences in behaviour of the signal gains. In the case of a CEC biosensor action, no notable amplification is observed in cases of a thin enzyme membrane ($d < 10^{-3}$ cm). A more distant increase of the thickness causes an increase of the gain G_{CEC}. The thickness at which G_{CEC} starts to increase, depends on the maximal enzymatic rate V_2.

The response of amperometric biosensors is known to be under mass-transport control if the diffusion modulus σ^2 is greater than unity, otherwise the enzyme kinetics controls the response:

$$\sigma^2 = \frac{V_{max}d^2}{D_S K_M} \tag{32}$$

where V_{max} is the maximal enzymatic rate and K_M is the Michaelis constant. Since the diffusion coefficient D_S and $K_M = K_1 = K_2$ are constant in all our numerical experiments as defined in (30) and the behaviour of biosensors acting in a trigger mode is mainly determined by the enzymatic rate V_2, (Figs. 5 and 6) the thickness d_σ of the enzyme layer as a function of V_2 at which $\sigma^2 = 1$ has been introduced:

$$d_\sigma(V_2) = \sqrt{\frac{D_S K_2}{V_2}} = \sqrt{\frac{3 \times 10^{-13}}{V_2}} \tag{33}$$

Figure 8. The signal gains G_{CEC} (1-3) and G_{CCE} (4-6) versus the membrane thickness d at three maximal enzymatic rates V_2: 100 (1, 4), 10 (2, 5) and 1 (3, 6) nmol/(cm^{3}s); $V_1 = 1$ μmol/(cm^{3}s), $S_{0N} = 0.2$.

Comparing the value $d_\sigma(10^{-6}) \approx 5.5 \times 10^{-4}$ cm with the membrane thickness at which the gain G_{CEC} starts to increase $V_2 = 10^{-6}$ mol/(cm^{3}s), one can notice that the amplification becomes noticeable when the mass transport by diffusion starts to control the biosensor response. As one can see in Fig. 8, this effect is also valid for two other values of the maximal enzymatic rate V_2: 10 and 100 nmol/(cm^{3}s). However, this is valid in the case of the biosensor acting in the CEC mode only. In the case of CCE mode, the gain G_{CCE} increases notably with increase of the thickness d in the entire domain. G_{CCE} is approximately a linear increasing function of d. However, the real amplification takes place in cases of relatively thick membranes only, $G_{CCE} > 1$ if only $d > \approx 2d_\sigma$. As it was noticed above (see Fig. 6), the steady-state current of the biosensor acting in the CCE mode may be even significantly less than the steady-state current of the corresponding biosensor acting in the CE mode at the same conditions. In a case of a relatively thick enzyme membrane, the gain G_{CCE} equals approximately to G_{CEC}, $G_{CCE} \approx G_{CEC}$.

Using a computer simulation, we calculated more precisely the thickness d_G of the enzyme membrane at which $G_{CCE} = 1$ for different enzymatic rates V_2. Accepting $V_1 = 1$ μmol/(cm^{3}s) it was

found that $d_G \approx 0.0009$ at $V_2 = 100$, $d_G \approx 0.003$ at $V_2 = 10$, and $d_G \approx 0.009$ cm at $V_2 = 100$ nmol/(cm^{3}s). These values of the membrane thickness compare favourably with values of the thickness d_{max} at which the steady-state current as a function of the membrane thickness d gains the maximum [24]:

$$d_{max} = \frac{1}{1.5055}\sqrt{\frac{D_S K_M}{V_{max}}} \qquad (34)$$

Consequently, for a low substrate concentration the thickness d_G of the enzyme membrane at which $G_{CEC} = 1$ can be precisely enough expressed as $d_G \approx 1.5\, d_\sigma$, where d_σ was defined in (33). Additional calculations showed that this property is valid for wide ranges of both maximal enzymatic rates: V_1 and V_2, if only the normalized substrate concentration S_{0N} is less than unity.

The effect of the membrane thickness on the response time

For comparing the time of a steady-state amplified biosensor response with the steady-state time of the response without amplification, we introduce a prolongation (L) of the response time as a ratio of the steady-state time of the trigger biosensor to the steady-state time of the corresponding CE biosensor:

$$L_m(V_1,V_2) = \frac{T_m(V_1,V_2)}{T_{CE}(V_1)} = \frac{T_m(V_1,V_2)}{T_m(V_1,0)}, \quad m = \text{CEC, CCE} \qquad (35)$$

where $T_m(V_1, V_2)$ is the steady-state time of the triggering biosensor acting in mode m at the maximal activity V_i of the enzyme E_i, m = CEC, CCE, i = 1, 2, $T_{CE}(V_1)$ is the steady-state time of the corresponding CE biosensor at the maximal enzymatic rate V_1. Since the action of the CE biosensor can be simulated as an action of a CEC biosensor accepting $V_2 = 0$, we assume $T_{CE}(V_1) = T_{CEC}(V_1, 0)$.

Fig. 9 shows the change of the response time versus the membrane thickness d at $V_1 = 1$ μmol/(cm^{3}s) and different values of V_2. One can see in Fig. 9, in all the presented cases, the prolongation of the response time (L_{CEC} as well as L_{CCE}) is a non-monotonous function of the thickness d. A shoulder on curves is especially noticeable at high maximal enzymatic rates. A similar effect was noticed in the case of biosensors with substrate cyclic conversion [16] and during the oxidation of β-nicotinamide adenine dinucleotide (NADH) at poly(aniline)-coated electrodes [28].

In the cases of thin enzyme membranes ($d < 0.001$ cm), the prolongation of the response time is insignificant. However, increasing the membrane thickness, the response time prolongation increases up to 3.4 times in both modes: CEC and CCE.

In the case of the CEC mode, the slight influence of the maximal enzymatic rate V_2 on L_{CEC} can be noticed in Fig. 9, while no notable influence of V_2 on L_{CCE} is observed in the case of CCE action mode. Additional calculations showed that the response time prolongation slightly depends on the substrate concentration S_0 as well as the maximal activity V_1 of the enzyme E_1.
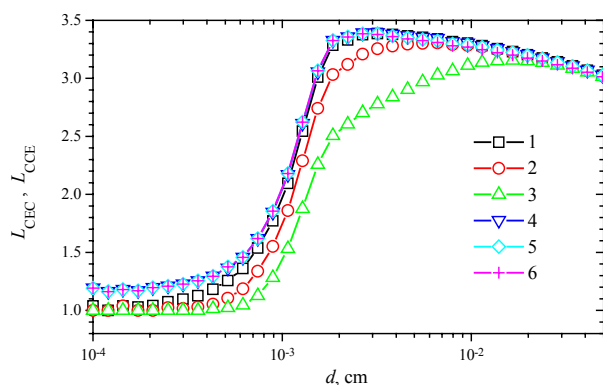
Figure 9. The increase of response time L_{CEC} (1-3) and L_{CCE} (4-6) versus the membrane thickness d. Parameters and notation are the same as in Fig. 8.

Conclusions

The mathematical model (4)-(13) of the biosensor action was used to investigate the dynamics of the response of biosensors utilizing a trigger enzymatic reaction followed by the electrochemical and enzymatic product cyclic conversion (CEC scheme (1)-(3)), while the model (19)-(21), (7)-(12), (22) was applied as a framework to investigate the behaviour of biosensors utilizing a trigger enzymatic reaction followed by the enzymatic and electrochemical conversion of the product (CCE scheme (16)-(18)).

The steady-state current I_{CEC} of a biosensor acting in the CEC mode and the steady state current I_{CCE} of a biosensor acting in the CCE mode are monotonous by increasing functions of both maximal enzymatic rates: V_1 and V_2 of enzymes E_1 and E_2, respectively (Figs. 3 and 4). The corresponding gains in sensitivity, G_{CEC} and G_{CCE}, of trigger biosensors were determined mainly by the enzymatic rate V_2 (Figs. 5 and 6). The enzymatic activity V_2 is a critical factor for the biosensor current in the case of CCE mode, $I_{CCE} \to 0$ as well as $G_{CCE} \to 0$ if $V_2 \to 0$. In the case of a CEC biosensor, the decrease of activity V_2 causes the decrease in gain G_{CEC}; however, G_{CEC} stays greater than unity, $G_{CEC} \to 1$ if $V_2 \to 0$.

Both signal gains, G_{CEC} and G_{CCE}, are most significant when the normalized concentration S_{0N} of the substrate is less than unity (Fig. 7). However, a stable and noticeable amplification (up to dozens of times) at a wide range of substrate concentration is achieved in the case of a relatively low maximal enzymatic activity (rate V_1) of enzyme E_1 and high activity (rate V_2) of enzyme E_2. In the cases of relatively high maximal enzymatic activity V_1, the signal amplification is stable only for low concentrations of the substrate.

In both biosensors acting modes, an insignificant amplification of the signal is observed if the diffusion modulus σ^2, calculated with the enzymatic rate V_2, is less than unity, i.e. the kinetics of enzyme E_2 controls the biosensor response. The gain G_{CCE} becomes even significantly less than unity if $\sigma^2 \ll 1$. For this type of biosensors, at a low substrate concentration, $S_{0N} < 1$, the gain G_{CCE} exceeds unity only when $\sigma > \approx 1.5$.

In the cases where the significant amplification of the signal of a triggering biosensor is achieved, the response time is up to several times longer than the response time of the corresponding biosensor acting without triggering (Fig. 9).

The models developed are permitted to build new trigger biosensors (in particular, by utilizing the CCE scheme). A highly sensitive hydrogen peroxide biosensor is under development and signal amplification has found the experimental confirmation.

Acknowledgements

References

1. Blaedel, W.J.; Boguslaski, R.C. A chemical amplification in analysis: a review. *Anal. Chem.* **1978**, 50, 1026.

2. Kulys, J. The development of new analytical systems based on biocatalysts. *Anal. Lett.* **1981**, 14 (B6), 377.

3. Schubert, F.; Kirstein, D.; Schröder, K.L.; Scheller, F. W. Enzyme electrodes with substrate and co-enzyme amplification. *Anal. Chim. Acta* **1985**, 169, 391.

4. Scheller, F.; Renneberg, R.; Schubert, F. Coupled enzyme reactions in enzyme electrodes using sequence, amplification, competition and anti-interference principles. In *Methods in Enzymology*; Academic Press: New York, **1988**; 137, 29.

5. Kulys, J.J.; Vidziunaite, R.A. Amperometric enzyme electrodes with chemically amplified response. In *Bioinstrumentation*; Wise, D.L., Ed.; Butterwoths, **1990**, 1263.

6. Wollenberger, U.; Lisdat, F.; Scheller, F.W. *Frontiers in Biosensorics 2, Practical Applications*; Birkhauser Verlag: Basel, **1997**.

7. Streffer, K.; Kaatz, H.; Bauer, C.G.; Makower, A.; Schulmeister, T.; Scheller, F.W.; Peter, M.G.; Wollenberger, U. Application of a sensitive catechol detector for determination of tyrosinase inhibitors. *Anal. Chim. Acta* **1998**, 362, 81.

8. Fuhrmann, B.; Spohn, U. An enzymatic amplification flow injection analysis (FIA) system for the sensitive determination of phenol. *Biosens. Bioelectron.* **1998**, 13, 895.

9. Kulys, J.J.; Sorochinski, V.V.; Vidziunaite, R.A. Transient response of bienzyme electrodes. *Biosensors* **1986**, 2, 135.

10. Schulmeister, T. Mathematical treatment of concentration profiles and anodic current of amperometric enzyme electrodes with chemically−amplified response. *Anal. Chim. Acta* **1987**, 201, 305.

11. Sorochinskii, V.V.; Kurganov, B.I. Steady−state kinetics of cyclic conversions of substrate in amperometric bienzyme sensors. *Biosens. Bioelectron.* **1996**, 11, 225.

12. Schulmeister, T.; Rose, J.; Scheller, F. W. Mathematical modelling of exponential amplification in membrane-based enzyme sensors. *Biosens. Bioelectron.* **1997**, 12, 1021.

13. Malinauskas, A.; Kulys, J. Alcohol, lactate and glutamate sensors based on oxidoreductases with regeneration of nicotinamide adenine dinucleotide. *Anal. Chim. Acta* **1978**, 98, 31.

14. Kulys, J.; Schmid, R.D. A sensitive enzyme electrode for phenol monitoring. *Analytical Letters* **1990**, 23(4), 589.

15. Kulys, J.; Vidziunaite, R. Amperometric biosensors based on recombinant laccases for phenols determination. *Biosens. Bioelectron.* **2003**, 18, 319.

16. Baronas, R.; Kulys, J.; Ivanauskas, F. Modelling amperometric enzyme electrode with substrate cyclic conversion. *Biosens. Bioelectron.* **2004**, 19, 915.

17. Della Ciana, L.; Bernacca, G.; Bordin, F.; Fenu, S.; Garetto, F. Highly sensitive amperometric measurement of alkaline phosphatase activity with glucose oxidase amplification. *J. Electronal. Chem.* **1995**, 382, 129.

18. Nistor, C.; Rose, A.; Wollenberger, U.; Pfeiffer, D.; Emnéus, J. A glucose dehydrogenase biosensor as an additional signal amplification step in an enzyme-flow immunoassay. *Analyst* **2002**, 127, 1076.

19. Razumas, V.J.; Kulys, J.J.; Malinauskas, A.A. Kinetic amperometric determination of hydrolase activity. *Anal. Chim. Acta* **1980**, 117, 387.

20. Crank, J. *The Mathematics of Diffusion*; 2nd ed., Clarendon Press: Oxford, **1975**.

21. Britz, D. *Digital simulation in electrochemistry*; 2nd ed., Springer−Verlag: Berlin, **1988**.

22. Bartlett, P.N.; Pratt, K.F.E. Modelling of processes in enzyme electrodes. *Biosens. Bioelectron.* **1993**, 8, 451.

23. Yokoyama, K.; Kayanuma, Y. Cyclic voltammetric simulation for electrochemically mediated enzyme reaction and determination of enzyme kinetic constants. *Anal. Chem.* **1998**, 70, 3368.

24. Baronas, R.; Ivanauskas, F.; Kulys, J. The influence of the enzyme membrane thickness on the response of amperometric biosensors. *Sensors* **2003**, 3, 248.

25. Ames, W.F. *Numerical Methods for Partial Differential Equations*; 2nd ed., Academic Press: New York, **1977**.

26. Press, W.H.; Flannery, B.P.; Teukolsky, S.A.; Vetterling, W.T. *Numerical Recipes in C: The Art of Scientific Computing*; Cambridge University Press: Cambridge, **1993**.

27. Turner, A.P.F.; Karube, I.; Wilson, G.S. *Biosensors: Fundamentals and Applications*; Oxford University Press: Oxford, **1987**.

28. Bartlett, P.N.; Birkin, P.R.; Wallace, E.N.K. Oxidation of β-nicotinamide adenine dinucleotide (NADH) at poly(aniline)-coated electrodes. *J. Chem. Soc., Faraday Trans.* **1997**, 93, 1951.